

Effect of stacking fault energy on nucleation limited plasticity in Cu-Al alloys

G. Kamalakshi, Prachi Limaye,
M.P. Gururajan and Prita Pant *

*Department of Metallurgical Engineering and Materials Science,
Indian Institute of Technology Bombay, Mumbai, India*

August 7, 2017

Abstract

We study the effect of Stacking Fault Energy (SFE) on the deformation behaviour of copper and copper-aluminium alloys using Molecular Dynamics (MD) simulation. We find that both yield stress and the magnitude of stress drop at yield decrease with increasing Al content. This anomalous softening behaviour is explained on the basis of nucleation controlled yielding behaviour. Further, the decrease in stress drop is rationalised in terms of the stored energy available at yielding we show that this decreases with increasing Al. As a result, the maximum dislocation density is found to decrease with increasing Al content.

1 Introduction

We are interested in studying the effect of Stacking Fault Energy (SFE) on deformation of single crystal fcc materials. Several Molecular Dynamics (MD) studies have been carried out to investigate the effect of SFE on plastic deformation in fcc metals [1–4] and alloys [5–10]. Of the studies on alloys, gold alloys are studied by nano-indentation [5], the studies on Ni-base superalloys are with specific reference to dislocation-solute interactions [8]; the studies on alloyed aluminium [6], Cu-Ag [9] and Cu-Pb [7] systems are on nanomaterials. Rajgharia et. al [10] have studied the effect of solute addition on tensile deformation of Cu-Sb single crystals; however, the amount of solute added and the corresponding change in SFE are very small (upto 2 at% and about 1 mJ/m², respectively). Our interest is to study the effect of a large change of SFE with alloying addition on tensile deformation in fcc single crystals (albeit simulated using periodic boundary conditions).

**Corresponding author. Email: pritapant@iitb.ac.in

We have chosen Cu-rich Cu-Al alloys (specifically, Cu-4.59at.%Al, Cu-8.94at.%Al and Cu-13.07at.%Al alloys) as the model system for our MD studies because the alloy remains as a single phase fcc upto about 13 at. %Al [11] and the SFE varies from about 43 mJ/m² for pure copper to about 6 mJ/m² for nearly 13 at.% Al alloy [12–16].

We find that in the nucleation limited systems, decreasing SFE with increasing solute content the onset of plastic deformation takes place at lower and lower stresses and the magnitude of the drop in stress at yield keeps decreasing. We show that this is due to the increasing ease of nucleation of loops of partial dislocations with decreasing SFE.

2 Simulation details

We have used LAMMPS [17] to carry out the MD simulations (of tensile deformation) using the Embedded Atom Method (EAM) potentials of Zhou and Ward [18]. All simulations are carried out at 300 K and 0 Pa (using an NPT ensemble); the temperature and pressure are maintained using Nosé-Hoover thermo- and baro-stats respectively. The temperature is ramped from 100 K to 300 K for the simulations.

We have used a simulation box of $30 \times 30 \times 30$ unit cells (108000 atoms) along x, y and z axes with periodic boundary conditions in all three directions; the x, y and z axes of the simulation cell are oriented along [100], [010] and [001] crystallographic directions respectively and the loading is done along the z-axis. After several trials, we have found that a strain rate of 10^8 s^{-1} is optimal since it leads to the required strains after about 15 million time steps and does not result in unphysical fluctuations in the stress-strain plot. The reported values of elastic moduli, yield stress, and drop at yield point, are based on an average of three simulations.

We have calculated the components of the stiffness tensor (that is, C_{11} , C_{12} and C_{44} since we are working with a cubic system) and lattice parameters for pure Cu and the Cu-Al alloys at 300 K. The elastic constants are calculated using the *change box* command of LAMMPS as indicated in the solved example [19], and the values are given in Table. 1 along with the lattice parameters.

The microstructures and dislocation structures are analysed using Ovito [20].

Table 1: Lattice parameter (a) and the elastic constants (C_{11} , C_{12} and C_{44}) of Cu and Cu-Al alloys.

System	a (\AA)	C_{11} (GPa)	C_{12} (GPa)	C_{44} (GPa)
Pure Cu	3.612 \pm 0.0	201.34 \pm 0.00	126.11 \pm 0.00	79.52 \pm 0.00
Cu-4.59at.%Al	3.626 \pm 0.0	160.83 \pm 0.40	121.86 \pm 0.07	69.59 \pm 0.25
Cu-8.94at.%Al	3.639 \pm 0.0	153.23 \pm 0.20	119.93 \pm 0.09	64.49 \pm 0.14
Cu-13.07at.%Al	3.652 \pm 0.0	145.87 \pm 0.47	117.02 \pm 0.52	59.83 \pm 0.82

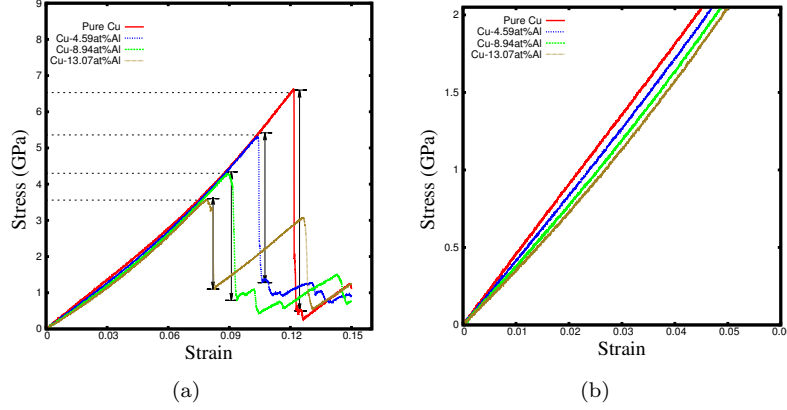


Figure 1: (a) Stress-strain response of Cu and Cu-Al alloys, black dotted lines show the yield point and black arrows show the amount of drop in stress at yield point. (b) Linear portion of the stress strain plot.

Table 2: Variation of yield stress, drop in stress ($\Delta\sigma$) and Youngs modulus (E) for Cu and Cu-Al alloys

Material	σ_y (GPa)	$\Delta\sigma$ (GPa)	E (GPa)
Cu	6.58 ± 0.02	6.08 ± 0.02	53.07 ± 0.16
Cu-4.59at.%Al	5.29 ± 0.04	4.22 ± 0.18	50.69 ± 0.24
Cu-8.94at.%Al	4.13 ± 0.16	3.29 ± 0.20	47.83 ± 0.30
Cu-13.07at.%Al	3.52 ± 0.05	2.45 ± 0.60	45.85 ± 1.59

3 Results and discussion

In Fig. 1, we show the stress-strain response for pure Cu, and Cu-4.59at.%Al, Cu-8.94at.%Al and Cu-13.07at.%Al alloys. In the inset, we also show the initial portion of the stress-strain plots from which it can be seen that the Young's modulus (E) decreases with increasing Al concentration; that is, the alloys are becoming less stiff with increasing Al. In the figure, in all plots, we have marked the first abrupt drop in stress by black dotted lines. At this point, as we show below, the onset of plasticity by nucleation of dislocation loops is seen. Hence, we call this stress as the yield stress, σ_y . The yield stress values decrease with increasing Al; further, the amount of drop in stress (indicated by black arrows) also decreases with increasing Al. In Table. 2, we have listed these yield stresses and the magnitude of drop in stress at these points. In other words, the addition of aluminium makes the material not only compliant but also soft.

3.1 Reasons for decreasing $\Delta\sigma$

It is easier to explain as to why $\Delta\sigma$ decreases with increasing Al. As the Al at.% increases, the alloys become more compliant; in addition, as we show below, it is also easier to initiate plastic deformation in them because of the reduced SFE; hence, they store relatively less elastic energy. We have calculated the slope of the stress-strain curves as the Youngs modulus (E). Based on these moduli, we have calculated the elastic energy as $\sigma_y^2/2E$ where σ_y is the yield stress. As shown in Fig. 2, the stored elastic energy at yield decreases with increasing Al. So, at the yield point, with increasing Al, the system has less and less energy to release in the form of dislocations; and, thus, the dislocation densities are expected to decrease with increasing Al content. In Fig. 2, we have also plotted the dislocation density after the first drop and this is indeed the case.

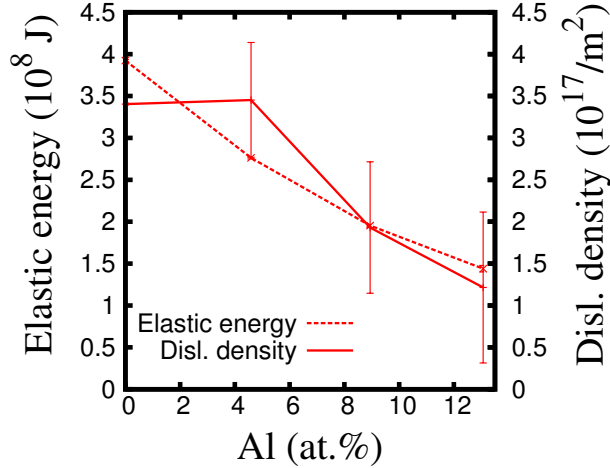


Figure 2: Variation of elastic energy and total dislocation density with Al.

3.2 Reasons for decreasing σ_y

Conventionally, the addition of a solute is expected to increase the yield stress in alloys [21–23]. In our case, we see an anomalous behaviour – namely, “solid solution softening”. We show below that this “softening” is due to the ease of formation of partial loops with increasing Al - because it leads to decreasing SFE.

Figures. 2.a-d, show the dislocation structure at the yield point for Cu and Cu-Al alloys. As is clear from these figures, in all cases, Shockley partial loops are formed. As a matter of fact, near the yield point, the ratio of the length of

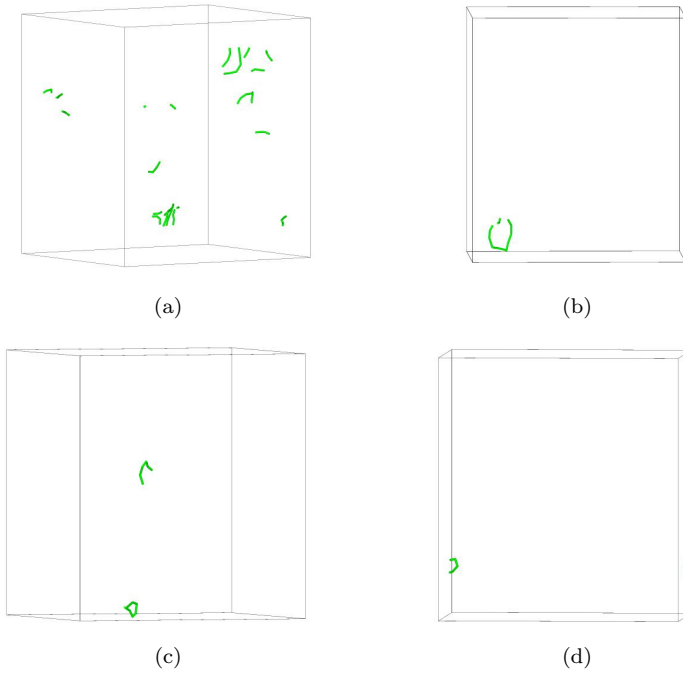


Figure 3: Nucleation of Shockley partial loop in (a) pure Cu, (b) Cu-4.59 at.% Al, (c) Cu-8.94 at.%Al and (d) Cu-13.07at.%Al. The ratios of the length of Shockley partial dislocations (L_S) to the length of total dislocations (L_T) near the drop for Cu, Cu-4.59 at.% Al, Cu-8.94 at.%Al and Cu-13.07at.%Al are 0.967 ± 0.024 , 0.997 ± 0.005 , 1.0 ± 0.0 and 0.991 ± 0.01 respectively.

Shockley partial dislocations (L_S) to total dislocation length (L_T) is found to be 0.95.

Given the predominance of Schockley partial dislocations in our MD simulations, we have used the continuum model proposed by Aubry et al [24] to estimate the stress required for the homogeneous nucleation of dislocation loops. In this model, the energy required for homogeneous nucleation of a partial dislocation loop (E_{nuc}) is given as follows:

$$E_{nuc}(\tau) = -b\tau A + \gamma_{SFE}A + 2\pi R \frac{\mu b^2}{8\pi} \left\{ \frac{2-\nu}{1-\nu} \left[\ln \left(\frac{8R}{r} \right) - 2 \right] + 0.5 \right\}, \quad (1)$$

where μ is the shear modulus (C_{44}), R the radius of the dislocation loop, A the area of the dislocation loop, b the Burgers vector of the Shockley partial ($\frac{1}{6}[11\bar{2}]$), ν the Poisson's ratio, r the dislocation core radius, γ_{SFE} the stacking fault energy and τ the applied shear stress. In Eq. 1, the first term is the elastic energy dissipated by the nucleation of a dislocation loop; the second term is the energy of the stacking fault created by the (partial) dislocation loop; and the third term is the elastic energy of the loop. The energy barrier for the dislocation nucleation is zero when the energy dissipated is equal to the sum of the energy of the (partial) dislocation loop and the stacking fault created by the loop. Therefore, the shear stress required for dislocation nucleation τ_{nuc} is obtained by equating Eq. 1 to zero:

$$\tau_{nuc} = \frac{\mu b}{4\pi R} \left\{ \frac{2-\nu}{1-\nu} \left[\ln \left(\frac{8R}{r} \right) - 2 \right] + 0.5 \right\} + \frac{\gamma_{SFE}}{b} \quad (2)$$

Note that in deriving the above expression, we have replaced A by πR^2 . Replacing μ by C_{44} and ν by $\frac{C_{12}}{C_{11}+C_{12}}$, Eq. 2 becomes:

$$\tau_{nuc} = \frac{C_{44}b}{4\pi R} \left\{ \frac{2C_{11}+C_{12}}{C_{11}} \left[\ln \left(\frac{8R}{r} \right) - 2 \right] + 0.5 \right\} + \frac{\gamma_{SFE}}{b}. \quad (3)$$

To evaluate the above expression, we have used the γ_{SFE} values reported in the literature and listed in Table. 3. The values of the elastic constants C_{11} , C_{12} and C_{44} and the Burgers vector (through the lattice parameters) are calculated using MD simulations and are listed in Table. 1. We have used the dislocation core radius (r) and radius of the dislocation loop (R) as fitting parameters. The τ_{nuc} values are calculated for (111) slip plane and $\frac{1}{6}[11\bar{2}]$ Burgers vector.

The tensile stress corresponding to τ_{nuc} was calculated for [001] loading direction using $\sigma_{nuc} = \tau_{nuc} \cos \phi \cos \lambda$ (where ϕ and λ are the angles made by the slip plane normal and the Burgers vector, respectively with the loading direction) and is given in column 4 of Table. 3. It is clear from the Table. 3 that, the tensile stress required for nucleation of partial dislocation decreases with increasing Al. In Table. 3, we also show the yield stress obtained from the MD simulations which agree fairly well with continuum calculations using the fitting parameters of $r = 3b = 0.442$ nm and $R = 2$ nm. The variation of yield stress with Al from the calculations and MD simulations is shown Fig. 4.

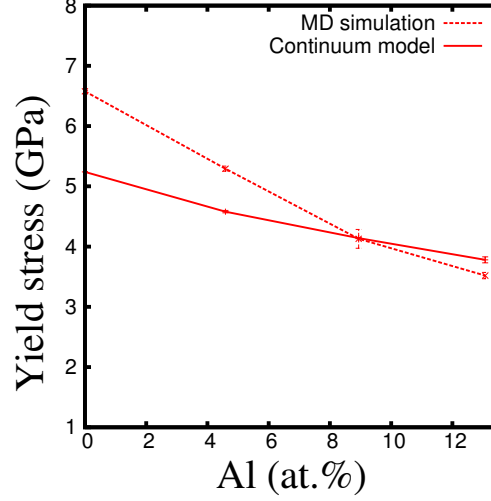


Figure 4: Change in yield stress with Al addition, calculated using continuum model [24] and obtained from MD simulations.

Table 3: Stress required for nucleation of partial dislocation with Burgers vector $\frac{1}{6}[11\bar{2}]$ in (111) plane for loading along $\langle 001 \rangle$ direction; σ_{nuc} is calculated from the continuum model and σ_y is obtained from MD simulations.

Material	γ_{SFE}	τ_{nuc}	σ_{nuc}	σ_y
Cu	43 [16]	2.47 ± 0.0	5.24 ± 0.0	6.58 ± 0.016
Cu-4.59%Al	25 [12]	2.16 ± 0.01	4.58 ± 0.02	5.29 ± 0.04
Cu-8.94%Al	13 [12]	1.95 ± 0.0	4.14 ± 0.01	4.13 ± 0.16
Cu-13.07%Al	6 [12]	1.78 ± 0.02	3.78 ± 0.05	3.52 ± 0.05

Solid solution softening has been reported in MD simulations of Cu-Pb system by Rupert [7], Cu-Ag system by Amigo et al [9], and Cu-Sb system by Rajgarhia et al [10]. Rupert reports that in nanocrystalline materials yield strength is proportional to the Young's modulus similar to the metallic glasses, and since the addition of Pb to Cu reduces the Young's modulus, the material shows softening behaviour. But our studies are on single crystals where no sources of dislocations such as grain boundaries exist; and so his explanation is not relevant for the system under study. Amigo et al and Rajgarhia et al [9, 10] find that the local strains created by the solute atoms lead to the heterogeneous nucleation of dislocations in their vicinity. However, in our study, we find nucleation both at Al sites and away from Al sites (even in systems with 4.93 and 8.94 at.% Al cases) – see Fig. 5; thus, we see both homogeneous and heterogeneous nucleation of dislocations and hence, the softening in our case can not be attributed to heterogeneous nucleation alone. Interestingly, we have found that in those studies in which the SFE of copper and aluminium was changed by using different interatomic potentials, as the SFE is decreased, the deformation is dominated by partials [1, 2]; specifically, in the case of copper bicrystals, the same trend, namely decrease in yield stress with decreasing SFE is observed.

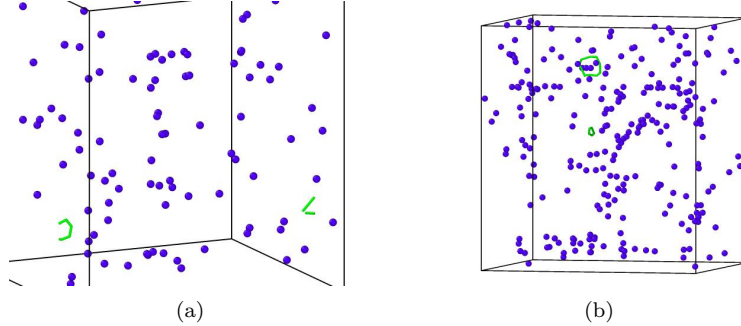


Figure 5: Nucleation of Shockley partials (shown in green – using dislocation analysis (DXA) of Ovito) in (a) Cu-4.59 at.% and (b) Cu-8.94 at.%Al systems. The blue circles are the Al atoms; for the sake of clarity, copper atoms are not shown. As is clear from the figure, both homogeneous and heterogeneous nucleation are seen.

4 Conclusion

The role of stacking fault energy on the deformation behaviour of Cu rich Cu-Al alloys, where SFE decreases with increasing Al content, is studied using molecular dynamics simulations. Since SFE decreases, it is easier for the system to nucleate partial dislocations; therefore, yield occurs at lower applied stress with increasing Al content. Because of decreasing Young's modulus and yield

stress, the system stores less elastic energy and hence the dislocation density decreases with Al addition. The yield stress values obtained from the simulations agree fairly well with the stress required for homogeneous nucleation of partials calculated using a continuum model.

4.1 Acknowledgements

We thank Mr. Saransh Singh and Dr. Arijit Roy for useful discussions; we thank Dendrite, Spinode – the DST-FIST HPC facility, and C-DAC, Pune for computational resources and DST, Government of India for funding this project (14DST017).

References

- [1] V. Borovikov, M.I. Mendelev, and A.H. King, *Effects of stable and unstable stacking fault energy on dislocation nucleation in nano-crystalline metals*, Modell. Simul. Mater. Sci. Eng. 24 (2016), pp. 85017–14.
- [2] T. Shimokawa, A. Nakatani, and H. Kitagawa, *Mechanical Properties Depending on Grain Sizes of Face-Centered-Cubic Nanocrystalline Metals Using Molecular Dynamics Simulation (Investigation of Stacking Fault Energy ' s Influence)*, JSME Int. J. 47 (2004), pp. 1708–1715.
- [3] H.S. Park, K. Gall, and J.A. Zimmerman, *Deformation of FCC nanowires by twinning and slip*, J. Mech. Phys. Solids 54 (2006), pp. 1862–1881.
- [4] V. Yamakov, D. Wolf, S.R. Phillpot, A.K. Mukherjee, and H. Gleiter, *Deformation-mechanism map for nanocrystalline metals by molecular- dynamics simulation*, Nat. Mater. 3 (2004), pp. 43–47.
- [5] Y. Li, A. Goyal, A. Chernatynskiy, J.S. Jayashankar, M.C. Kautzky, S.B. Sinnott, and S.R. Phillpot, *Nanoindentation of gold and gold alloys by molecular dynamics simulation*, Mater. Sci. Eng. A 651 (2016), pp. 346–357.
- [6] S. Hocker, M. Hummel, P. Binkele, H. Lipp, and S. Schmauder, *Molecular dynamics simulations of tensile tests of Ni-, Cu-, Mg- and Ti-alloyed aluminium nanopolycrystals*, Comp. Mater. Sci. 116 (2015), pp. 32–43.
- [7] T.J. Rupert, *Solid solution strengthening and softening due to collective nanocrystalline deformation physics*, Scripta Mater. 81 (2014), pp. 44–47.
- [8] X. Zhang, H. Deng, S. Xiao, X. Li, and W. Hu, *Atomistic simulations of solid solution strengthening in Ni-based superalloy*, Comp. Mater. Sci. 68 (2013), pp. 132–137.
- [9] N. Amigo, G. Gutiérrez, and M. Ignat, *Atomistic simulation of single crystal copper nanowires under tensile stress: Influence of silver impurities in the emission of dislocations*, Comp. Mater. Sci. 87 (2014), pp. 76–82.

- [10] R.K. Rajgarhia, D.E. Spearot, and A. Saxena, *Heterogeneous dislocation nucleation in single crystal copperantimony solid-solution alloys*, Modell. Simul. Mater. Sci. Eng. 17 (2009), pp. 55001–13.
- [11] B. Lu, K. Chen, and W.J. Meng, *Quantification of Thermal Resistance of Transient-Liquid- Phase Bonded Cu / Al / Cu Interfaces for Assembly of Cu-Based Microchannel Heat Exchangers*, J. Micro Nano-Manuf. 1 (2016), pp. 1–10.
- [12] A. Rohatgi, K.S. Vecchio, and G.T. Gray, *The influence of stacking fault energy on the mechanical behavior of Cu and Cu-Al alloys: Deformation twinning, work hardening, and dynamic recovery*, Metall. Mater. Trans. A 32 (2001), pp. 135–145.
- [13] M. Chassagne, M. Legros, and D. Rodney, *Atomic-scale simulation of screw dislocation/coherent twin boundary interaction in Al, Au, Cu and Ni*, Acta Mater. (2011), pp. 1456–1463.
- [14] Z.X. Wu, Y.W. Zhang, and D.J. Srolovitz, *Dislocation twin interaction mechanisms for ultrahigh strength and ductility in nanotwinned metals*, Acta Mater. 57 (2009), pp. 4508–4518.
- [15] M.D. Sangid, T. Ezaz, and H. Sehitoglu, *Energetics of residual dislocations associated with slip twin and slip GBs interactions*, Mater. Sci. Eng. A 542 (2012), pp. 21–30.
- [16] C.B. Carter and I.L.F. Ray, *On the stacking-fault energies of copper alloys*, Philos. Mag. 35 (1977), pp. 189–200.
- [17] S. Plimpton, *Fast Parallel Algorithms for Short-Range Molecular Dynamics*, J. Comput. Phys. 117 (1995), pp. 1–19, Available at <http://lammps.sandia.gov>.
- [18] L. Ward, A. Agrawal, K.M. Flores, and W. Windl, *Rapid Production of Accurate Embedded Atom Method Potentials for Metal Alloys*, Model. Simul. Mater. Sc. (2012).
- [19] A. Thompson. Available at <http://lammps.sandia.gov/doc/Sectionexample.html>.
- [20] A. Stukowski, *Visualization and analysis of atomistic simulation data with OVITO the Open Visualization Tool*, Modelling Simul. Mater. Sci. Eng. 18 (2009), pp. 015012–7, Available at <http://ovito.org/>.
- [21] G.E. Dieter, *Mechanical Metallurgy*, 3rd ed., McGraw Hill Education (India) Private Limited, New Delhi, 2016.
- [22] T.H. Courtney, *Mechanical Behavior of Materials*, 2nd ed., McGraw Hill Custom Pub., United States of America, 2000.

- [23] M.A. Meyers and K.K. Chawla, *Mechanical Behavior of Materials*, 2nd ed., Cambridge University Press, New York, 2009.
- [24] S. Aubry, K. Kang, S. Ryu, and W. Cai, *Energy barrier for homogeneous dislocation nucleation: Comparing atomistic and continuum models*, Scripta Mater. (2011), pp. 1043–1046.